Distortion-Loop Analysis for Full-Duplex Amplify-and-Forward Relaying in Cooperative Multicast Scenarios

Omid Taghizadeh*, Markus Rothe*, Ali Cagatay Cirik† and Rudolf Mathar*
* Institute for Theoretical Information Technology, RWTH Aachen University, Aachen, 52074, Germany
† Institute for Digital Communications, University of Edinburgh, Edinburgh EH9 3JL, U.K
Email: taghizadeh@ti.rwth-aachen.de, rothe@ti.rwth-aachen.de, a.cirik@ed.ac.uk, mathar@ti.rwth-aachen.de

***Abstract*—In this work we study the behavior of a full-duplex (FD) and amplify-and-forward (AF) relay where realistic limitations of FD relays in overcoming their loopback self-interference signal are taken into account. This includes the inaccuracies of the analog hardware components, as well as the limited interference estimation accuracy in the baseband (digital) domain. As it will be elaborated, due to the inter-dependency of the transmit relay power and the residual self-interference in an AF-FD relay, we observe a distortion loop that dominates the system performance when the relay dynamic range is not adequately high. The effects of this loop are then studied analytically and the optimal relay selection and power optimization is derived, assuming a setup with a single source and multiple destination nodes (multicast scenario). In order to provide further intuition, system behavior and the corresponding optimal designs are studied analytically for few extreme cases. In particular, a comparison is made with the similar relaying setup with decode-and-forward (DF) process, where the distortion loop is reduced due to decoding. Finally, the gains of the proposed design as well as the effect of different system parameters are investigated via numerical simulations.**

I. Introduction

The idea of full-duplex (FD) operation, as transceiver's capability to transmit and receive at the same time and frequency, is known with the potential to approach various requirements of future communication systems (5G), e.g., improving spectral efficiency, physical layer security and reduced end-to-end latency [1], [2]. Nevertheless, such systems have been long considered to be practically infeasible due to the inherent self-interference. In theory, since each node is aware of its own transmitted signal, the interference from the loopback path can be estimated and suppressed. However, in practice this procedure is challenging due to the high strength of the self-interference channel compared to the desired communication path, up to 100 dB [3]. Recently, specialized cancellation techniques [4]–[8] have provided an adequate level of isolation between Tx and Rx directions to facilitate a FD communication, and motivated wide range of related applications, e.g., [3], [9]–[16]. A common idea of these techniques is the accurate attenuation of main interference paths in RF (prior to down-conversion), so that the remaining self-interference can be correctly processed in the effective dynamic range of the analog-to-digital convertor (ADC) and further attenuated in the baseband (digital) domain. While the aforementioned cancellation techniques have provided successful demonstrations for specific scenarios, e.g., [7], it is easy to observe that the obtained cancellation level may vary for various realistic conditions. This mainly includes i) aging and inaccuracy of the analog components, e.g., ADC and digital-to-analog-convertor (DAC), power amplifier and oscillator in the analog domain, as well as ii) inaccurate estimation of the remaining interference paths due to the limited channel coherence time, noise and limited processing power in digital domain. As a result, this is essential to correctly model and take into account the aforementioned inaccuracies to obtain a design which remains efficient under realistic situations.

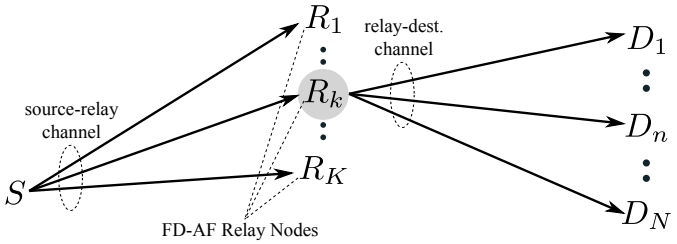

Fig. 1. The signal flow as described in Section II. Transmitted signal from source (S) is forwarded by the selected relay (distinguished with gray shadow) to the destination nodes.

In this work we are focusing on the application of FD capability on the classic relaying systems, where the source node communicates with multiple destination nodes with the help of a relay. Benefiting from the broadcast nature of the wireless channels, multicast communication is deployed for the multi-user and group communication scenarios were multiple nodes receive the same message without burdening the network with multiple retransmissions, see [17]–[19]. A FD relay is capable of receiving the signal from the source, while simultaneously communicating to the destination. This capability, not only reduces the required time slots in order to accomplish an end to end communication, but also reduces the end to end latency compared to the traditionally Time Division Duplex (TDD)-based half-duplex (HD) relays. The design methodologies and performance evaluation for FD relays with DF operation have been studied in [11] and [20] by incorporating the aforementioned cancellation inaccuracies, and also in [12], [21] with a threshold-based approach towards the suppressible self-interference power. For the systems with AF-FD relays the system behavior results in a rather com-

plicated mathematical description. This stems from the inter-dependent behavior of the transmit power from the relay and the residual self-interference components, which result in a distortion loop, see Subsection II-C. As a result, simplified models are widely used for related investigations. The design methodologies for AF-FD relaying systems have been studied in [22], [23] assuming perfect self-interference cancellation, in [24], [25] assuming conditional perfect cancellation with a threshold for the allowed self-interference power, and in [26] assuming a known variance for residual self-interference at the relay. The above-mentioned studies, while providing a smart trade-off between design complexity and system performance, may lead to inefficient design due to the non-realistic assumptions. In few works that apply a more accurate model, a power-constraint relaying with single user communication is studied in [27]–[29]. In the aforementioned works the effect of inaccurate interference estimation in digital domain have been incorporated in [28], where the distortions from analog domain components have been addressed in [27], following the experimental modeling [30]–[32] and in [29] following the proposed model in [33]. The work in [29] is then extended by [34] to enhance the physical layer secrecy in the presence of an Eavesdropper.

While the aforementioned literature introduces the importance of more accurate transceiver modeling for AF-FD relays, only few relaying scenarios have been so far studied in this scope. Furthermore the previous works lack elaboration on the aforementioned distortion loop, and how it affects the performance of an AF-FD relay. In particular, a comparison with an equivalent DF-FD relay is essential for each scenario, where this loop can be significantly alleviated as the received signal is decoded prior to amplification and transmission.

Contribution: In this paper we extend the work in [27] to the scenario where the analog domain inaccuracies in the receiver chain, the transmitter chain, as well as digital domain self-interference channel estimation errors are jointly taken into account. A setup with a single source and multiple destination nodes (multicast) is studied in order to generalize our analysis into a broader range of wireless communication applications, see [17]–[19]. The optimal relay selection and amplification strategies are then derived analytically. This is done by assuming a norm-2 ball for the feasible self-interference channel estimation error, and optimizing the worst-case end-to-end performance, corresponding to the worst-case estimation error. In order to provide a better intuition, system behavior and the corresponding optimal designs are then studied analytically for few extreme scenarios where the system performance is dominated with noise, or with distortion components. A comparison is then made with a similar setup with a DF-FD relay, where the studied distortion loop is alleviated via decoding. Finally, the gains of the proposed design as well as the effect of different system parameters are investigated via numerical simulations.

Paper organization: In this document we provide a detailed system model in Section II. Optimal relay amplification and selection is then derived in Section III. The behavior of the system for few extreme cases is analyzed in Section IV. A comparison between AF-FD and DF-FD relaying schemes is done in Section V, and finally, the proposed solutions are evaluated via numerical simulations in Section VI.

TABLE I. LIST OF THE USED SYMBOLS IN THE DEFINED SYSTEM

Notation	Description
s, P_s	transmit signal from the source and its power
$h_{\mathrm{sr},k}$	channel coefficient for the source-relay paths
$h^{(n)}_{\mathrm{rd},k}$	channel coefficient for the relay-destination paths
$h_{\mathrm{rr},k}$	channel coefficient for the self-interference paths
$\tilde{h}_{\mathrm{rr},k}$	estimated self-interference channel coefficient
δ_k	self-interference channel estimation error
$\mathcal{H}_k$	set of all feasible self-interference channel estimation errors
$\delta_k^\star$	the worst-case feasible $\delta_k \in \mathcal{H}_k$
γ_k, β_k	ratio representing Tx and Rx chain's dynamic range
a_k	relay amplification coefficient
m_k, M_k	the additive white noise at R_k and its variance
$w^{(n)}, W^{(n)}$	the additive white noise at D_n and its variance
$e_{\mathrm{in},k}, e_{\mathrm{out},k}$	error signals originating from Rx and Tx chains
$r_{\mathrm{in},k}, r_{\mathrm{out},k}$	input and output signals at R_k
$u_{\mathrm{in},k}, u_{\mathrm{out},k}$	non-distorted received and transmit signals at R_k
P_k	maximum individual allowed power
$\mathbb{S}_K, \mathbb{S}_N$	index set of respectively all relay and destination nodes

II. SYSTEM MODEL

We investigate the scenario where a HD single antenna source (S) multicasts a message to N single antenna destinations ($D_1 \cdots D_N$) with the help of an AF relay node (Fig.1). We assume there exist K relay nodes ($R_1 \cdots R_K$) from which the best relay will be selected to forward the message to the destination nodes. Relay nodes are equipped with single transmit (Tx) and single receive (Rx) antenna and operate in FD mode, i.e., reception from the source and transmission to the destination nodes are performed simultaneously. All communication channels are assumed to follow the block flat-fading model. We denote the channel between S and R_k as $h_{\mathrm{sr},k} \in \mathbb{C}$ and the channel between R_k and D_n as $h^{(n)}_{\mathrm{rd},k} \in \mathbb{C}$, where k, n respectively represent the index of the corresponding relay and destination nodes. The loopback self-interference channel for R_k is denoted as $h_{\mathrm{rr},k} \in \mathbb{C}$. Due to the high strength of the self-interference channel, only an estimate of the self-interference channel, i.e., $\tilde{h}_{\mathrm{rr},k}$, is known. Hence the accurate self-interference channel coefficient can be written as

$$h_{\mathrm{rr},k} = \tilde{h}_{\mathrm{rr},k} + \delta_k, \quad \delta_k \in \mathcal{H}_k,$$
$$\mathcal{H}_k := \{\forall \delta_k \in \mathbb{C} \mid |\delta_k|_2 \leq \zeta_k\},$$

where $\delta_k \in \mathbb{C}$ is the channel estimation error and $\mathcal{H}_k$ is a confidence set, which contains the values of δ_k with a high probability. The value $\zeta_k \in \mathbb{R}^+$ represents the radius of the confidence set, and depends on the quality of the channel estimation. More elaborations on the aforementioned channel estimation error model and the choice of confidence set is given in [35]. In this work the path between the source and destination nodes are assumed to be ignorable. The index set of all relay nodes in the network is denoted as $\mathbb{S}_K$ while the index set of all destination nodes is denoted as $\mathbb{S}_N$.

A. Source-to-relay communication

Upon selection of the k-th relay node, R_k, it continuously receives and amplifies the received signal from the source, while dealing with the loopback self-interference signal from its own transmitter front-end, see Fig. 2. This is done by

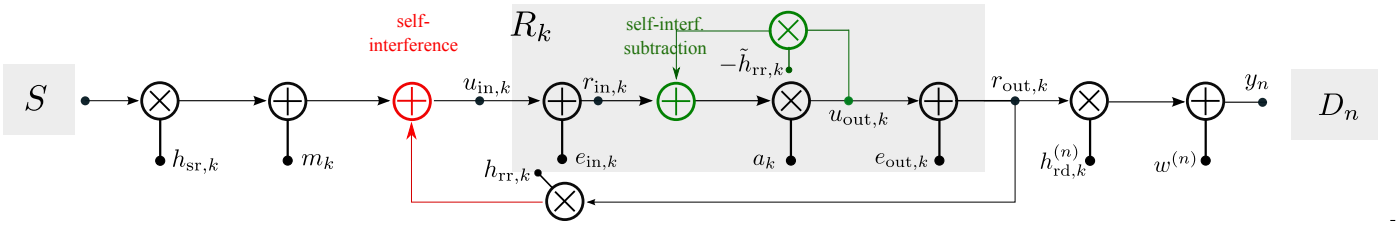

Fig. 2. The interaction of different signal components in an amplify-and-forward FD relay node. The loopback-self interference affects the residual interference intensity. The red signal represents the self-interference signal while the green signal represents the suppressible (estimated) interference part.

utilizing the known self-interference cancellation techniques, e.g., [5]–[7], in the receiver front-end. The received signal on the relay is

$$r_{\mathrm{in},k} = \underbrace{h_{\mathrm{sr},k}\cdot s + \tilde{h}_{\mathrm{rr},k}\cdot r_{\mathrm{out},k} + \delta_k \cdot r_{\mathrm{out},k} + m_k}_{=:u_{\mathrm{in},k}} + e_{\mathrm{in},k}, \tag{1}$$

where $r_{\mathrm{in},k}, r_{\mathrm{out},k} \in \mathbb{C}$ respectively represent the received and transmitted signal at the k-th relay node and $m_k \in \mathbb{C}$ represents the zero-mean circularly symmetric complex Gaussian (ZMCSCG) noise with variance M_k. The transmitted signal from the source is represented as $s \in \mathbb{C}$ and $u_{\mathrm{in},k} \in \mathbb{C}$ is the *undistorted* received signal on the Rx antenna. The receiver distortion, as the additional error from antenna up to ADC module is represented as $e_{\mathrm{in},k} \in \mathbb{C}$, which represents the effect of limited dynamic range (e.g., limited ADC accuracy) in facing with the high-power received signal. For detailed elaboration on this distortion model please refer to [11], [32] and system measurements in [30], [31]. While the aforementioned error is assumed to be ignorable in many classic HD schemes, it plays an important role in our system due to the high power nature of the self-interference. The known (distortion-free) part of the self-interference signal is then suppressed and the resulting signal is amplified to constitute the relay's output: [1]

$$r_{\mathrm{out},k} = \underbrace{a_k \cdot r_{\mathrm{supp},k}}_{=:u_{\mathrm{out},k}} + e_{\mathrm{out},k}, \tag{2}$$

$$r_{\mathrm{supp},k} = r_{\mathrm{in},k} - \tilde{h}_{\mathrm{rr},k}\cdot u_{\mathrm{out},k}, \tag{3}$$

where $r_{\mathrm{supp},k} \in \mathbb{C}$ and $a_k \in \mathbb{C}$ represent the interference-suppressed version of the received signal and the amplification coefficient at R_k. The *intended* transmit signal is denoted as $u_{\mathrm{out},k}$. Similar to the defined distortion in the receiver chain, we define the transmitter distortion as $e_{\mathrm{out},k}$ which represents the effect of limited transmitter dynamic range, [11], [32]. As it has been shown, the variance of the distortion components is proportional to the collected power on the receiver antenna (undistorted received signal), for $e_{\mathrm{in},k}$, and to the power of the transmit signal prior to DAC module (intended Tx signal), for $e_{\mathrm{out},k}$:

$$\mathcal{E}\{e_{\mathrm{in},k}e^*_{\mathrm{in},k}\} = \beta_k \cdot \mathcal{E}\{u_{\mathrm{in},k}{u_{\mathrm{in},k}}^*\}, \quad \forall k \in \mathbb{S}_K, \tag{4}$$

$$\mathcal{E}\{e_{\mathrm{in},k}e^*_{\mathrm{in},l}\} = 0, \quad k \neq l, \tag{5}$$

$$\mathcal{E}\{e_{\mathrm{out},k}e^*_{\mathrm{out},k}\} = \gamma_k \cdot \mathcal{E}\{u_{\mathrm{out},k}{u_{\mathrm{out},k}}^*\}, \quad \forall k \in \mathbb{S}_K, \tag{6}$$

$$\mathcal{E}\{e_{\mathrm{out},k}e^*_{\mathrm{out},l}\} = 0, \quad k \neq l, \tag{7}$$

where $\mathcal{E}\{\cdot\}$ represents the mathematical expectation and $\beta_k, \gamma_k \in \mathbb{R}^+$ are coefficients respectively relating the *intended* receive and transmit signal power to the variance of the resulting distortion. The transmit power of the relay node is limited by

$$\mathcal{E}\{r_{\mathrm{out},k}r^*_{\mathrm{out},k}\} \leq P_k, \quad k \in \mathbb{S}_K, \tag{8}$$

where P_k represents the maximum allowed power on the function of R_k.

B. Relay-to-destination communication

The transmitted signal from the selected relay node, R_k, passes through the relay to destination channels and constitutes the received signal at the destination nodes:

$$y^{(n)} = h^{(n)}_{\mathrm{rd},k}\cdot r_{\mathrm{out},k} + w^{(n)}, \tag{9}$$

where $y^{(n)}, w^{(n)} \in \mathbb{C}$ respectively represent the received signal at D_n, and the ZMCSCG noise with variance $W^{(n)}$. Table I provides the description of the signal notations to better communicate the defined model.

C. Distortion loop

In this part we provide an intuitive description of the aforementioned distortion loop, following the defined system model, which makes the subsequent arguments in the paper more clear. As the transmit power from the relay increases, the power of the error components, both due to analog and digital domain errors increase, see (1) in connection to (4)-(7). On the other hand, these errors are amplified in the relay process and further increase the relay transmit power, see (1) in connection to (2) and (3). The aforementioned effect causes a loop which signifies the problem of residual self-interference for the relays with AF process. In the following section, we study the problems regarding optimal relay selection and the optimal choice of relay amplification coefficients for the defined system.

III. Optimal Relay Selection for Full-Duplex Amplify-and-Forward Relays

In this section we obtain an optimal relay selection strategy together with the optimal relay amplification coefficients, following the max-min approach. This leads to the maximum end to end communication rate which is preserved for all multicast destination nodes, and for all feasible self-interference channel estimation errors defined by the sets $\mathcal{H}_k$. Due to the single stream setup we equivalently define our problem as

Signal-to-Error-plus-Noise-Ratio (SENR) maximization at the destination nodes. This can be hence formulated as

$$\max_{k\in\mathbb{S}_K,\, a_k\in\mathcal{A}_k} \Big\{ \min_{n\in\mathbb{S}_N,\, \delta_k\in\mathcal{H}_k} \mathrm{SENR}_k^{(n)} \Big\}, \tag{10}$$

where $\mathcal{A}_k$ includes all values of a_k which satisfy the R_k transmit power constraint (8), and $\mathrm{SENR}_k^{(n)}$ is the resulting SENR at D_n if R_k is selected as the active relay node. In order to solve the above problem, in the first step, we derive an explicit formulation for the relay's transmit power which plays an important role in the formulation of SENR values. By incorporating (1), (4)-(7) into (2) and (3) we have [1]

$$\begin{aligned}\mathcal{E}\{u_{\mathrm{out},k}u_{\mathrm{out},k}^*\} &= |a_k|^2 \Big(P_s\,|h_{\mathrm{sr},k}|^2 + M_k + \mathcal{E}\{e_{\mathrm{in},k}e_{\mathrm{in},k}^*\} \\ &+ \mathcal{E}\{e_{\mathrm{out},k}e_{\mathrm{out},k}^*\}\cdot|h_{\mathrm{rr},k}|^2 + \mathcal{E}\{r_{\mathrm{out},k}r_{\mathrm{out},k}^*\}\cdot|\delta_k|^2\Big) \\ &= |a_k|^2 \Bigg(P_s\,|h_{\mathrm{sr},k}|^2 + M_k + \mathcal{E}\{u_{\mathrm{in},k}u_{\mathrm{in},k}^*\}\beta_k \\ &+ \mathcal{E}\{u_{\mathrm{out},k}u_{\mathrm{out},k}^*\}\cdot\Big(|h_{\mathrm{rr},k}|^2\gamma_k + (1+\gamma_k)|\delta_k|^2\Big)\Bigg), \end{aligned} \tag{11}$$

where $P_s := \mathcal{E}\{ss^*\}$ is the transmit power from the source. The undistorted received power at the relay can be calculated from (1)-(3) as

$$\mathcal{E}\{u_{\mathrm{in},k}u_{\mathrm{in},k}^*\} = P_s\,|h_{\mathrm{sr},k}|^2 + M_k + |h_{\mathrm{rr},k}|^2\,\mathcal{E}\{r_{\mathrm{out},k}r_{\mathrm{out},k}^*\}. \tag{12}$$

It is worth mentioning that due to the proximity of the Rx and Tx antennas on the FD device, the loopback self-interference signal is much stronger than the desired signal which is coming from a distant location, e.g., up to 100 dB according to [6], and hence constitutes the principle part in (12). By incorporating (12) into (11) and recalling (6) and (2) we have

$$\begin{aligned}&\mathcal{E}\{r_{\mathrm{out},k}r_{\mathrm{out},k}^*\} \\ &\quad= (\gamma_k+1)\cdot\mathcal{E}\{u_{\mathrm{out},k}u_{\mathrm{out},k}^*\} \\ &\quad= \frac{(\eta_k+1)\,|a_k|^2\Big(P_s\,|h_{\mathrm{sr},k}|^2 + M_k\Big)}{1-|a_k|^2\Big(\,|h_{\mathrm{rr},k}|^2\,\eta_k + (\gamma_k+1)\,|\delta_k|^2\Big)}, \end{aligned} \tag{13}$$

where $\eta_k := \gamma_k + \beta_k + \gamma_k\beta_k$. Note that the above derivations (11)-(13) hold given that all components of the desired signal (s), noise (m_k) and the distortion components ($e_{\mathrm{in},k}, e_{\mathrm{out},k}$) are zero mean and mutually independent. In order to obtain an explicit formulation for $\mathrm{SENR}_k^{(n)}$, we distinguish the desired as well as the error plus noise parts of the signal power at the destination. By exploiting the independence among noise, error and desired signal components we have

$$P_{\mathrm{desired},k}^{(n)} = P_s\cdot|a_k|^2\left|h_{\mathrm{sr},k}h_{\mathrm{rd},k}^{(n)}\right|^2 \tag{14}$$

$$\begin{aligned}P_{\mathrm{destructive},k}^{(n)} &= \left|h_{\mathrm{rd},k}^{(n)}\right|^2\Big(\mathcal{E}\{r_{\mathrm{out},k}r_{\mathrm{out},k}^*\} \\ &\quad - P_s\,|h_{\mathrm{sr},k}|^2\cdot|a_k|^2\Big) + W^{(n)}, \end{aligned} \tag{15}$$

[1]The relay output signals, i.e., $u_{\mathrm{out},k}$ and $r_{\mathrm{out},k}$, are generated from the received signals in the previous symbol duration. The subsequent communicated symbols are assumed zero-mean and independent. The time (symbol) index is eliminated to simplify the notations.

where $P_{\mathrm{desired},k}^{(n)}, P_{\mathrm{destructive},k}^{(n)}$ respectively represent the power of the desired and destructive parts of the signal at D_n.

Lemma 1: The worst-case $\delta_k \in \mathcal{H}_k$, denoted as $\delta_k^\star$, given the self-interference channel estimation $\tilde{h}_{\mathrm{rr},k}$ is calculated as $\delta_k^\star = \frac{\zeta_k\tilde{h}_{\mathrm{rr},k}}{|\tilde{h}_{\mathrm{rr},k}|}$.

Proof: It is apparent from (14) and (15) that the desired power is invariant to the choice of δ_k. On the other hand, the value of $P_{\mathrm{destructive},k}^{(n)}$ is monotonic with respect to the transmit power from the relay. Hence, the worst-case δ_k is the one that minimizes the denominator in (13), or equivalently maximizes the term: $|\tilde{h}_{\mathrm{rr},k}+\delta_k|^2\eta_k + (\gamma_k+1)\,|\delta_k|^2$. This results in the $\delta_k \in \mathcal{H}_k$ with maximum amplitude, and with similar phase as $\tilde{h}_{\mathrm{rr},k}$, i.e., $\delta_k^\star = \frac{\zeta_k\tilde{h}_{\mathrm{rr},k}}{|\tilde{h}_{\mathrm{rr},k}|}$. ∎

The value of $\mathrm{SENR}_k^{(n)}$ is then formulated in (16) assuming R_k is active with an arbitrary amplification coefficient (a_k), and self-interference channel estimation error δ_k. As it is clear from (16), the phase of a_k has no effect on the resulting SENR. Hence we consider $\tilde{a}_k := |a_k|^2$ as our optimization parameter hereinafter. As it is formulated in (10), our goal is to maximize the worst-case link quality in the defined multicast system. The weakest link quality, denoted as $\tilde{\mathrm{SENR}}_k$ hereafter, can be hence formulated as a function of the selected relay and the corresponding amplification coefficient in (17) and consequently as (18). This is done by applying Lemma 1, and factoring the common channel coefficient $h_{\mathrm{rd},k}^{(n)}$ from nominator and denominator of (16). It is important to note that while the value of $\tilde{\mathrm{SENR}}_k$ approaches zero for $\tilde{a}_k \to 0$ and $\tilde{a}_k \to \tilde{a}_k^\infty$ ($\tilde{a}_k^\infty := \frac{1}{b_k}$, see (18)), it remains positive and differentiable on all values in the range $(0, \tilde{a}_k^\infty)$. By incorporating (8), and observing the fact that $\mathcal{E}\{r_{\mathrm{out},k}r_{\mathrm{out},k}^*\}$ is monotonically increasing in $\tilde{a}_k$, the feasible region for $\tilde{a}_k$ is determined as $\tilde{a}_k \in [0, \tilde{a}_{k,\max}]$, where

$$\begin{aligned}\tilde{a}_{k,\max} := P_k\cdot\Big((1+\eta_k)\Big(P_s\,|h_{\mathrm{sr},k}|^2 + M_k\Big) \\ + P_k b_k\Big)^{-1},\ \ 0 \le \tilde{a}_{k,\max} < \tilde{a}_k^\infty. \end{aligned} \tag{19}$$

Note that the identity (18) holds for all feasible a_k as $\tilde{\mathrm{SENR}}_k$ remains differentiable and continuous within the region $0 \le \tilde{a}_k \le \tilde{a}_{k,\max}$. The problem of maximizing the minimum link quality for a given selected relay can be hence formulated as

$$\begin{aligned}&\max_{\tilde{a}_k}\ (18), \\ &\text{s.t. } 0 \le \tilde{a}_k \le \tilde{a}_{k,\max}. \end{aligned} \tag{20}$$

By taking the derivative, the stationary points of the objective function can be achieved as

$$\begin{aligned}r_{k,1} &= \frac{-1}{c_k - b_k} + \frac{\sqrt{c_k/b_k}}{|c_k - b_k|}, \\ r_{k,2} &= \frac{-1}{c_k - b_k} - \frac{\sqrt{c_k/b_k}}{|c_k - b_k|}, \end{aligned} \tag{21}$$

where $b_k := |\tilde{h}_{\mathrm{rr},k} + \delta_k^\star|^2\eta_k + (\gamma_k+1)\,|\delta_k^\star|^2$ and $c_k := \frac{(1+\eta_k)\left(P_s|h_{\mathrm{sr},k}|^2+M_k\right)}{\ell_k} \in \mathbb{R}^+$.

$$\mathrm{SENR}_k^{(n)} = \frac{P_{\mathrm{desired},k}^{(n)}}{P_{\mathrm{destructive},k}^{(n)}} = \frac{P_s \cdot |a_k|^2 \left|h_{\mathrm{sr},k} h_{\mathrm{rd},k}^{(n)}\right|^2}{\left|h_{\mathrm{rd},k}^{(n)}\right|^2 \left(\frac{(\eta_k+1)|a_k|^2\left(P_s|h_{\mathrm{sr},k}|^2+M_k\right)}{1-|a_k|^2\left(|h_{\mathrm{rr},k}|^2\eta_k+(\gamma_k+1)|\delta_k|^2\right)} - P_s\,|h_{\mathrm{sr},k}|^2 \cdot |a_k|^2\right) + W^{(n)}}, \tag{16}$$

$$\tilde{\mathrm{SENR}}_k := \min_{n\in\mathbb{S}_N,\ \delta_k\in\mathcal{H}_k} \mathrm{SENR}_k^{(n)} = \min_{n\in\mathbb{S}_N} \left\{ \frac{P_s\tilde{a}_k\,|h_{\mathrm{sr},k}|^2}{\frac{(1+\eta_k)\tilde{a}_k\left(P_s|h_{\mathrm{sr},k}|^2+M_k\right)}{1-\tilde{a}_k b_k} - P_s\,|h_{\mathrm{sr},k}|^2\cdot\tilde{a}_k + W^{(n)}/|h_{\mathrm{rd},k}^{(n)}|^2} \right\} \tag{17}$$

$$= \frac{P_s\tilde{a}_k\,|h_{\mathrm{sr},k}|^2}{\frac{(1+\eta_k)\tilde{a}_k\left(P_s|h_{\mathrm{sr},k}|^2+M_k\right)}{1-\tilde{a}_k b_k} - P_s\,|h_{\mathrm{sr},k}|^2\cdot\tilde{a}_k + \ell_k}, \tag{18}$$

where $\eta_k := \gamma_k + \beta_k + \beta_k\gamma_k$, $b_k := |\tilde{h}_{\mathrm{rr},k} + \delta_k^\star|^2\eta_k + (\gamma_k+1)|\delta_k^\star|^2$, $\ell_k := \max\limits_{n\in\mathbb{S}_N}\left\{W^{(n)}/|h_{\mathrm{rd},k}^{(n)}|^2\right\}$, $\tilde{a}_k := |a_k|^2$.

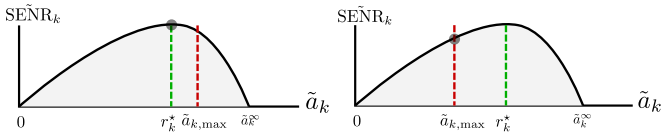

(a) $r_k^\star \le \tilde{a}_{\max,k}$ (b) $r_k^\star > \tilde{a}_{\max,k}$

Fig. 3. Possible situations of $r^\star$ considering the feasible region of $\tilde{a}_k$. The dark circle indicates the position of the optimum point.

Lemma 2: The values of $r_{k,1}, r_{k,2}$ are real for the defined system. Moreover, there exists exactly one extremum for $\tilde{\mathrm{SENR}}_k$ in the range $\tilde{a}_k \in (0, \tilde{a}_k^\infty)$. This extremum is a maximum and obtained as the smallest non-negative value among $r_{k,1}, r_{k,2}$. We name this value as $r_k^\star$ hereinafter.

Proof: Since $b_{k,1}, b_{k,2} \in \mathbb{R}^+$, the real-valued nature of $r_{k,1}, r_{k,2}$ can be directly concluded from (21). On the other hand, the value of $\tilde{\mathrm{SENR}}_k$ approaches to zero as $\tilde{a}_k \to 0$ and $\tilde{a}_k \to \tilde{a}_k^\infty$, for nonzero values of noise and distortion components. Since the value of $\tilde{\mathrm{SENR}}_k$ remains positive, continues and differentiable in the range $(0, \tilde{a}_k^\infty)$ there exists at least one maximum in this region. In this regard, two scenarios are probable. If $0 < b_{k,1} < b_{k,2}$, then $r_{k,2} < 0$ and $r_{k,1}$ is the only extrema in the positive region. On the other hand, if $b_{k,1} > b_{k,2} > 0$ we have $r_{k,1}, r_{k,2} \in \mathbb{R}^+$. In this case we have

$$r_{k,1} = \frac{1}{b_{k,1}-b_{k,2}} + \frac{\sqrt{b_{k,2}/b_{k,1}}}{|b_{k,2}-b_{k,1}|} > \frac{1}{b_{k,1}-b_{k,2}} > \frac{1}{b_{k,1}} = \tilde{a}_k^\infty.$$

The above argument concludes that we never face with two stationary points in the region $(0, \tilde{a}_k^\infty)$, and the only root which is located in the aforementioned region, is the single SENR-maximizing point we have been looking for, i.e., $r_k^\star$. ∎

The above Lemma leaves us with $\tilde{a}_k = r_k^\star$ as the SENR-maximizing point in the region $(0, \tilde{a}_k^\infty)$. If $r_k^\star \le \tilde{a}_{k,\max}$ (feasibility condition), then $r_k^\star$ represents the value of optimal $\tilde{a}_k$, see Fig. 3-a. On the other hand, since the $\tilde{\mathrm{SENR}}_k$ function has no other extrema in the aforementioned region, if $r_k^\star > \tilde{a}_{k,\max}$ then $\tilde{\mathrm{SENR}}_k$ is an increasing function of $\tilde{a}_k$ inside its feasible region. In such a case, the optimal $\tilde{a}_k$ is located on the boundary of the feasible region where $\tilde{a}_k$ holds the maximum feasible value, see Fig. 3-b. Hence we always achieve the optimal $\tilde{a}_k$ as

$$\tilde{a}_k^\star = \min\left\{r_k^\star, \tilde{a}_{k,\max}\right\}, \quad a_k^\star = \sqrt{\tilde{a}_k^\star}, \tag{22}$$

where $a_k^\star$ represents the optimum relay amplification coefficient, assuming that R_k is selected as the active relay. It is worth mentioning that due to the single operation of the relay node, the phase of $a_k^\star$ does not affect the objective as it is clear from (17), (18). The corresponding minimum link quality is then calculated via (18) and the relay node which offers the highest minimum link quality, will be the selected relay to forward the message from the source. The performance of the defined FD relaying together with the obtained optimal design is demonstrated in Section VI with respect to different system parameters.

A. Computational Complexity

It should be noted that while the proposed design is based on further knowledge of the loopback interference path and gathering the data to a centralized node, it does not add a significant solution complexity in comparison to the traditional designs with simplified distortion models. From (22) and the formulation in (21), the overall required design computation is calculated as $2N + 21K$ floating-point operations (FLOPs). The aforementioned amount is very small, in comparison with the capability of the commonly used processors.

As we have observed from above analysis, while the efficiency of the FD relaying can be increased due to simultaneous transmission and reception, the system behavior is different from the previous HD schemes due to the nature of the resulting residual interference. In the following we study the resulting system behavior for two extreme scenarios.

IV. System Behavior in Extreme Scenarios

In this part we investigate the behavior of the optimal design for different special cases. In particular, we investigate the case where the distortion components at the FD relay nodes are negligible due to the sufficient precision of the hardware components, as well as the case where the noise power is ignorable at the destination nodes. The aforementioned scenarios respectively correspond to the FD system with high dynamic range and the system which operates in a high SNR region.

A. Special case: $W^{(n)} \to 0,\ M_k \to 0$

This scenario corresponds to the case where the receiver thermal noise floor is ignorable compared to the incoming

signal power at the receiver ends. By applying the above assumptions to (16) we formulate the corresponding SENR values as

$$\min_{n\in\mathbb{S}_N} \ \mathrm{SENR}_k^{(n)} = \frac{P_s\cdot|a_k|^2\,|h_{\mathrm{sr},k}|^2}{\frac{(1+\eta_k)|a_k|^2P_s|h_{\mathrm{sr},k}|^2}{1-|a_k|^2b_k} - P_s\,|h_{\mathrm{sr},k}|^2\cdot|a_k|^2} = \frac{1}{\frac{(1+\eta_k)}{1-|a_k|^2b_k}-1}. \tag{23}$$

As it is clear, (23) is monotonically decreasing in $\tilde{a}_k$ in the feasible range. Hence as the value of $\tilde{a}_k$ approaches zero, the resulting $\mathrm{SENR}_k^{(n)}$ corresponding to the weakest link approaches to $\frac{1}{\eta_k} = (\beta_k+\gamma_k+\beta_k\gamma_k)^{-1}$ as the upper bound to the optimal achievable minimum SENR. Nevertheless, this value may never be achieved in practice as the presence of any noise components results in zero SENR at the destination nodes for an extremely small choice of $\tilde{a}_k$. We recall that in the current scenario, the performance is limited only by the effects of limited system dynamic range (i.e. inaccuracies in ADC, DAC, ...) and limited digital domain estimation accuracy, excluding the effect of the thermal noise on the receiver front end.

B. Special case: $\beta_k, \gamma_k, \zeta_k \to 0$

This case corresponds to a FD system with accurate function of the involved transceiver components. In practice this can be approached by using more accurate elements in the system (e.g., ADC module with higher resolution) and effective passive isolation between Tx and Rx which alleviates the effects of distortion components. In this scenario the SENR formulation is significantly simplified and second order terms at the denominator of (18) disappear:

$$\min_{n\in\mathbb{S}_N,\ \delta_k\in\mathcal{H}_k} \ \mathrm{SENR}_k^{(n)} = \frac{P_s\cdot\tilde{a}_k\,|h_{\mathrm{sr},k}|^2}{\tilde{a}_kM_k+\ell_k}, \tag{24}$$

which is a monotonically increasing function with respect to $\tilde{a}_k$ and results in the maximum amplification at the relay in the optimum point. We should note that this is the similar problem structure to the equivalent HD system, where the self-interference does not exist at the relays [36]. Nevertheless, higher efficiency is achieved due to FD operation at the relay nodes, which results in doubling the achievable communication rate.

C. System behavior interpretation

As we have observed, the two aforementioned extreme scenarios lead to opposite optimal designs in terms of transmit power. In the first case, where system performance is dominated by the distortion components, the system tends to consume a very small power at the relay node. Furthermore, increasing the transmit power from the source doesn't affect the resulting performance bound, which is obtained as $\frac{1}{\eta_k}$. On the other hand, the maximum relay power is used in the second case where distortion components are ignored and system performance is limited by noise. In this case, increasing P_s results in the higher link quality. As it is partly described in Section II, the opposite behavior of the aforementioned cases stems from the fact that the variance of the distortion components, unlike the noise components, are dependent on the Tx and Rx signal power at the corresponding chain, see Fig. 2. Unlike the HD scenario where the maximum transmit power is used at optimality, this observation reveals the significance of power optimization at the FD relays, prior to relay selection.

V. Amplify-and-Forward vs. Decode-and-Forward FD Relaying Under Residual Self-Interference

In this part, we study the performance of the defined system, assuming the relay decodes the interference-suppressed received signal, r_{supp}, prior to amplification. We assume a single relay, single destination system, i.e., $K=1,\ N=1$, and drop the indexes k, n from the notations in this section, for simplicity. As the result (2) can be formulated as

$$r_{\mathrm{out}} = a\cdot\rho\big(r_{\mathrm{supp}}\big)+e_{\mathrm{out}}, \tag{25}$$

where $\rho(\,\cdot\,)$ represents the decoding process in the relay. The end-to-end rate of the relay channel can be written as [37], [38]

$$R_{\text{s-d}} = \min\big(R_{\text{s-r}}, R_{\text{r-d}}\big), \tag{26}$$

where $R_{\text{s-d}}, R_{\text{s-r}}, R_{\text{r-d}}$ respectively represent the communication rates corresponding to the source-to-destination, source-to-relay, and the relay-to-destination paths. Assuming Gaussian distribution for the source signal, noise and distortion components, we can formulate an equivalent SENR form of (26) as

$$R_{\text{s-d}} = \log_2\Big(1+\min\big(\omega_{\text{s-r}},\omega_{\text{r-d}}\big)\Big), \tag{27}$$

$$\omega_{\text{s-r}} \approx \frac{P_s\,|h_{\mathrm{sr}}|^2}{b\tilde{a}+M},\ \ \omega_{\text{r-d}} \approx \frac{\tilde{a}\,|h_{\mathrm{rd}}|^2}{W}, \tag{28}$$

where $\omega_{\text{s-r}}$ and $\omega_{\text{r-d}}$ are the resulting SENR in the source-to-relay and relay-to-destination paths. The noise variance at the relay and destination are denoted as M, and W, and $\tilde{a} := |a|^2$ and $b := |\tilde{h}_{\mathrm{rr}}+\delta^\star|^2\eta+(\gamma+1)|\delta^\star|^2$, see (18). Note that assuming $\mathcal{E}\{ss^*\}=1$, the relay's transmit power can be closely approximated as $\tilde{a}$. In the current setup, due to the single relay operation, the resulting SENR is invariant to the phase of the amplification coefficients. As it can be observed from (28), the value of $\omega_{\text{s-r}}$ is monotonically decreasing, and $\omega_{\text{r-d}}$ is monotonically increasing with respect to $\tilde{a}$. Hence the maximum $R_{\text{s-d}}$ occurs either as the relay power constraint is tight, or as the values of $\omega_{\text{r-d}}$ and $\omega_{\text{s-r}}$ are equal. In this way we have

$$\tilde{a}^\star = \min\left(P_{\max}, -\frac{M}{2b}+\sqrt{\frac{M^2}{4b^2}+\frac{WP_s\,|h_{\mathrm{sr}}|^2}{b\,|h_{\mathrm{rd}}|^2}}\right),$$
$$a^\star = \sqrt{\tilde{a}^\star}\,\angle\theta, \tag{29}$$

where the angle θ can be chosen arbitrarily, and $a^\star$ represents the optimal relay amplification assuming the DF relay strategy, following (25). Consequently, the resulting end-to-end rate corresponding to (28) and (27) represents the achievable rate with DF relaying strategy.

A. Distortion loop in DF-FD relays

As we recall for an AF-FD relay, the behavior of distortion loop is grounded in the dependency of the transmit power to the residual self-interference power, and simultaneously the dependence of the relay transmit power to the power of the residual interference components. As it is apparent, due to the decoding process such a dependency does not exist for a regenerative relaying scheme and hence the corresponding performance degradation is avoided for a DF-FD relay. This can be mathematically seen from the linear dependency of error variance in the denominators in (28), compared to the denominator in (18).

In Section VI, a numerical comparison is made between the performance of the FD relays, applying DF and AF strategies and the obtained optimal performance under residual interference, i.e., (22) and (29).

VI. Simulation Results

In this part, we investigate the behavior of the proposed optimal designs via Monte Carlo simulations. We assume all channels follow the uncorrelated Rayleigh flat-fading model, and average the results over 1000 channel realizations. The resulting minimum end-to-end rate, corresponding to the weakest source-to-destination link and the worst-case channel estimation error for the defined multicast system is depicted in Figs. 4-7. In Fig. 4 the proposed optimal design in Section III is applied to study the system performance for different parameters. As it is observed, the resulting system performance is significantly dependent on the noise levels at the destination and at the relay nodes, $W_n = W,\ \forall n \in \mathbb{S}_N$, $M_k = M,\ \forall k \in \mathbb{S}_K$, number of relay and destination nodes, K, N, and the distortion levels at the Rx and Tx chains, $\beta_k = \beta,\ \gamma_k = \beta,\ \forall k \in \mathbb{S}_K$. Unless otherwise stated we choose $\gamma = \beta = -40\,\text{dB}$, $K = 10$, $N = 10$, $W = M = -40\,\text{dBW}$, $P_s = P_k = 0\,\text{dBW}$, and $\mathcal{E}\{|h_{\text{rr},k}|\} = 0\,\text{dB}$, $\mathcal{E}\{|h_{\text{sr},k}|\} = \mathcal{E}\{|h^{(n)}_{\text{rd},k}|\} = -30\,\text{dB}$, $\forall k \in \mathbb{S}_K, n \in \mathbb{S}_N$ as the default values for our system parameters. On the other hand, in order to observe the significance of the power optimization with accurate modeling of the transmit and receive chains imperfections, we provide a comparison between the proposed optimal design, and the available solutions in Figs. 5-7. The resulting minimum end-to-end rate, corresponding to the weakest link and the worst-case channel estimation error is illustrated for different noise and distortion and channel estimation inaccuracy levels. 'Optimal' represents the proposed design in Section III for optimal relay selection and power adjustment. 'Maximum Amplification' method simplifies the results of Section III by using the maximum feasible amplification in the relay as the transmission and selection strategy, see (19). 'Random Sel' represents the method where the selection is done randomly among the available relays, and 'Simplified Model' refers to the method using the applied model in [26] where the residual self-interference is treated as an additional noise component with a known variance, σ^2_{int}. The significant performance gain compared to the traditional designs is observed in Fig. 6. This is expected, recalling the opposite nature of the optimal solution compared to the traditional design for high SNR regions which is discussed in Section IV. In Fig. 8 a comparison is made for a single relay,

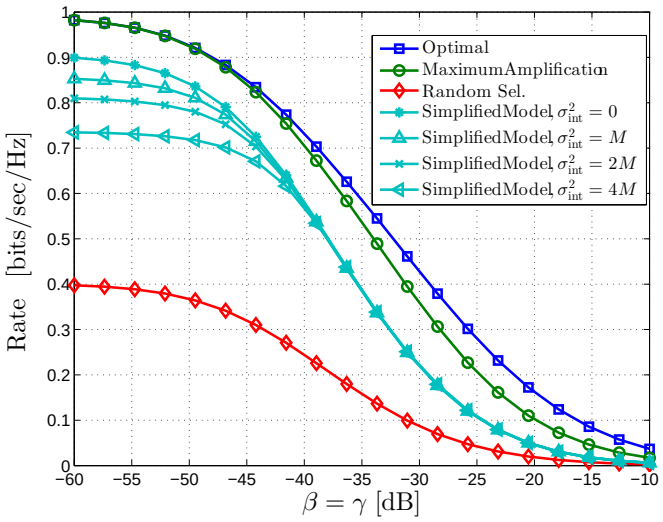

Fig. 5. Achievable rate [bits/sec/Hz] for the weakest end-to-end link vs. distortion coefficients η, β [dB]. The gain is observed specially for low dynamic range region. $\zeta_k = 0$.

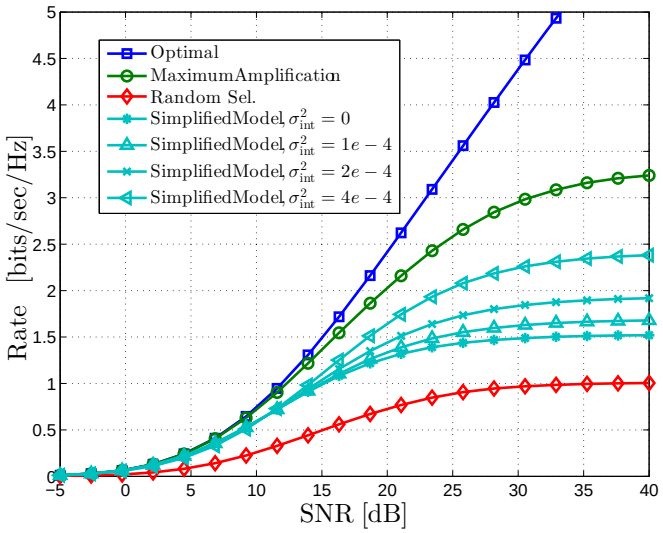

Fig. 6. Achievable rate [bits/sec/Hz] for the weakest end-to-end link vs. SNR [dB]. The significant gain is observed for the optimal design in high SNR region. $\text{SNR} := \frac{P_s \mathcal{E}\{|h_{\text{sr},k}|^2\}}{M}$, $\zeta_k = 0$.

single destination system between DF-FD and AF-FD relaying schemes in the presence of distortion loop. The decoding gain is observed over various noise and distortion intensities. The distortion coefficient b includes the combined effect of the inaccuracies in the Tx/Rx chain components, as well as the worst-case self-interference channel estimation, see (18). The obtained optimal designs are applied for both relaying schemes to perform a fair comparison, see (22) and (29). In Fig. 9 the relative gain of a DF-FD relay, i.e., $\frac{R_{\text{DF}} - R_{\text{AF}}}{R_{\text{AF}}}$ where R_{DF} and R_{AF} represent the obtained rate for DF and AF cases, is observed. As it is shown, as the relative gain remains constant and small where the system performance is dominated with noise (the effect of distortion loop is ignorable, similar to HD setup), as the distortion components become dominant this

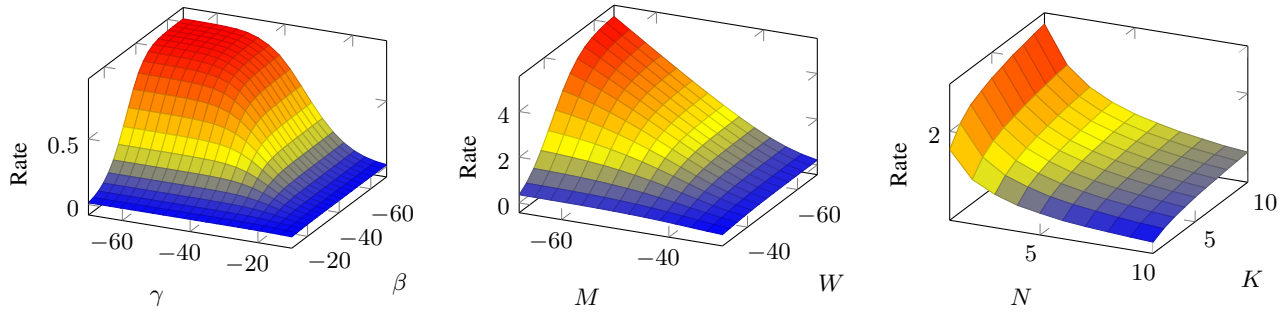

Fig. 4. The achievable rate [bits/sec/Hz] for the weakest end-to-end link with the proposed optimal design vs. system noise levels M, W [dBW], distortion intensity, γ, β [dB], and the number of relay and destination nodes, K, N.

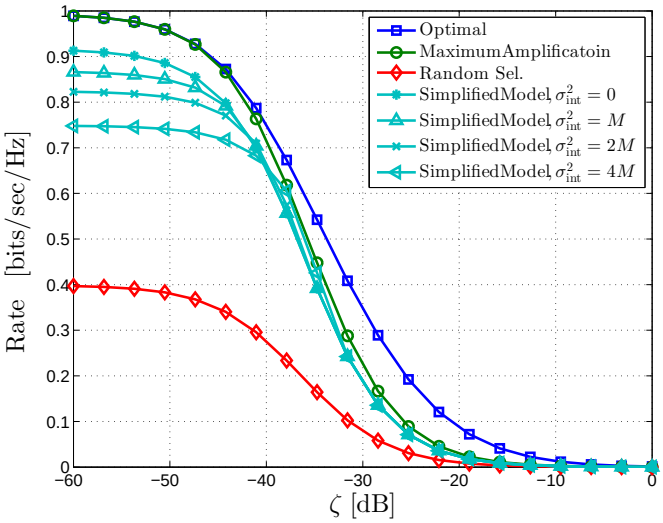

Fig. 7. Achievable rate [bits/sec/Hz] for the weakest end-to-end link vs. radius of the feasible channel estimation error set, i.e., $\mathcal{H}_k$, where $\zeta = \zeta_k, \forall k$, $\eta = \beta = 0$. A relatively similar effect is observed compared to the distortion components, as they both result in higher residual interference at the relay.

ratio increases dramatically. This effect, once again, reinforces the consideration of the resulting distortion loop, as described earlier.

VII. Conclusion

It is already known that for a system with FD operation, the performance can be degraded due to the residual self-interference, remaining from the self-interference cancellation process. In this work, we have shown that a FD and non-regenerative (AF) relaying system suffers additionally from a distortion loop, connecting the power of the transmit signal to the residual interference components: As the transmit power from the relay increases, the resulting inaccuracies increase both in Tx and Rx chains. These inaccuracies remain as residual interference components, which are then amplified in the relaying process and further increase the transmit power. In this work, we have analytically studied the effects of this power loop, for a relaying system with multiple destinations. We have particularly observed how the aforementioned effect deviates the optimal design structure from the traditional designs where simplified assumptions are used. The significance of the studied effect has been further observed by a comparison between the defined AF-FD relaying setup to a DF-FD counterpart, where the distortion loop can be alleviated via decoding. The simulation results in Section VI, as well as the analysis in Section IV, reinforce the importance of the proposed approach.

References

[1] J. I. Choi, S. Hong, M. Jain, S. Katti, P. Levis, and J. Mehlman, "Beyond full duplex wireless," in *Forty Sixth Asilomar Conference on Signals, Systems and Computers*, Nov 2012.

[2] S. Hong, J. Brand, J. Choi, M. Jain, J. Mehlman, S. Katti, and P. Levis, "Applications of self-interference cancellation in 5G and beyond," *IEEE Communications Magazine*, February 2014.

[3] B. Day, A. Margetts, D. Bliss, and P. Schniter, "Full-duplex bidirectional MIMO: Achievable rates under limited dynamic range," *IEEE Transactions on Signal Processing*, Jul. 2012.

[4] D. Korpi, S. Venkatasubramanian, T. Riihonen, L. Anttila, S. Otewa, C. Icheln, K. Haneda, S. Tretyakov, M. Valkama, and R. Wichman, "Advanced self-interference cancellation and multiantenna techniques for full-duplex radios," in *Signals, Systems and Computers, 2013 Asilomar Conference on*, Nov 2013.

[5] M. Jain, J. I. Choi, T. Kim, D. Bharadia, K. Srinivasan, S. Seth, P. Levis, S. Katti, and P. Sinha, "Practical, real-time, full duplex wireless," in *Proceedings of 17th Annual International Conference on Mobile Computing and Networking (MobiCom)*, Las Vegas, NV, Sep. 2011.

[6] Y. Hua, P. Liang, Y. Ma, A. Cirik, and G. Qian, "A method for broadband full-duplex MIMO radio," *IEEE Signal Processing Letters*, vol. 19, Dec. 2011.

[7] D. Bharadia, E. McMilin, and S. Katti, "Full duplex radios," in *Proceedings of the ACM SIGCOMM*, Aug. 2013.

[8] A. K. Khandani, "Two-way (true full-duplex) wireless," in *13th Canadian Workshop on Information Theory (CWIT, 2013)*.

[9] A. Cirik, R. Wang, Y. Hua, and M. Latva-aho, "Weighted sum-rate maximization for full-duplex mimo interference channels," *Communications, IEEE Transactions on*, vol. 63, March 2015.

[10] A. Cirik, Y. Rong, and Y. Hua, "Achievable rates of full-duplex MIMO radios in fast fading channels with imperfect channel estimation," *Signal Processing, IEEE Transactions on*, vol. 62, no. 15, Aug 2014.

[11] B. Day, A. Margetts, D. Bliss, and P. Schniter, "Full-duplex MIMO relaying: Achievable rates under limited dynamic range," *IEEE Journal on Selected Areas in Communications*, Sep. 2012.

[12] O. Taghizadeh and R. Mathar, "Full-duplex decode-and-forward relaying with limited self-interference cancellation," in *Proceedings of International ITG Workshop on Smart Antennas (WSA), Erlangen, Germany*, March 2014.

[13] T. Riihonen, S. Werner, and R. Wichman, "Transmit power optimization for multiantenna decode-and-forward relays with loopback self-interference from full-duplex operation," *Proc. 45th Annual Asilomar*

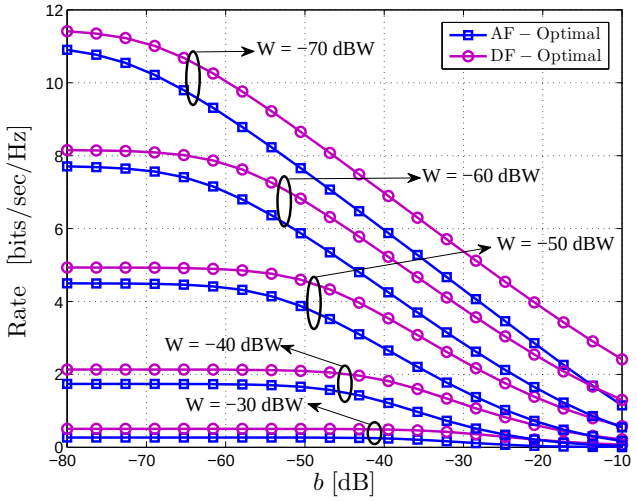

Fig. 8. Achievable rate [bits/sec/Hz] for the vs. b [dB], for optimal DF and AF relaying in different noise regimes. b represents the inaccuracy of self-interference cancellation, see (18). $W = M$ represents the different noise levels. $K = N = 1$.

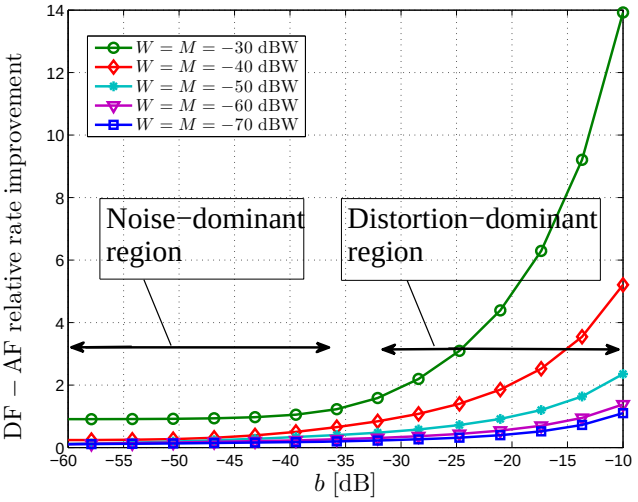

Fig. 9. Relative rate improvement in DF-FD relay compared to AF-FD scheme vs. b [dB]. b represents the inaccuracy of self-interference cancellation, see (18). The relative gain increases dramatically as the distortion loop gets stronger. $K = N = 1$.

Conference on Signals, Systems, and Computers, Pacific Grove, CA, 2010.

[14] G. Zheng, I. Krikidis, J. Li, A. Petropulu, and B. Ottersten, "Improving physical layer secrecy using full-duplex jamming receivers," *IEEE Transactions on Signal Processing*, Oct 2013.

[15] O. Taghizadeh and R. Mathar, "Interference mitigation via power optimization schemes for full-duplex networking," in *19th International ITG Workshop on Smart Antennas*, March 2015.

[16] J. Zhang, O. Taghizadeh, and M. Haardt, "Robust transmit beamforming design for full-duplex point-to-point MIMO systems," *Proceedings of the Tenth International Symposium on Wireless Communication Systems (ISWCS)*, Aug. 2013.

[17] K. Elkhalil, M. Eltayeb, H. Shibli, H. Bahrami, and T. Al-Naffouri, "Opportunistic relay selection in multicast relay networks using compressive sensing," in *Global Communications Conference (GLOBECOM), 2014 IEEE*, Dec 2014.

[18] M. Khandaker and Y. Rong, "Precoding design for mimo relay multicasting," *Wireless Communications, IEEE Transactions on*, July 2013.

[19] J. Joung, H. D. Nguyen, P. H. Tan, and S. Sun, "Multicast linear precoding for mimo-ofdm systems," *Communications Letters, IEEE*, June 2015.

[20] E. Antonio-Rodriguez, R. Lopez-Valcarce, T. Riihonen, S. Werner, and R. Wichman, "Sinr optimization in wideband full-duplex mimo relays under limited dynamic range," in *Sensor Array and Multichannel Signal Processing Workshop (SAM), 2014 IEEE 8th*, June 2014.

[21] O. Taghizadeh and R. Mathar, "Robust multi-user decode-and-forward relaying with full-duplex operation," in *The Eleventh International Symposium on Wireless Communication Systems (ISWCS 2014)*, Barcelona, Spain, Sep. 2014.

[22] K. Lee, H. Kwon, M. Jo, H. Park, and Y. Lee, "MMSE-based optimal design of full-duplex relay system," in *IEEE Vehicular Technology Conference (VTC Fall)*, Sept 2012.

[23] H. Maier and R. Mathar, "Cyclic interference neutralization on the full-duplex relay-interference channel," in *IEEE International Symposium on Information Theory (ISIT)*, Istanbul, Turkey, Jul. 2013, pp. 2409–2413.

[24] Y. Y. Kang, B.-J. Kwak, and J. H. Cho, "An optimal full-duplex AF relay for joint analog and digital domain self-interference cancellation," *IEEE Transactions on Communications*, Aug 2014.

[25] J. Zhang, O. Taghizadeh, and M. Haardt, "Joint source and relay precoding design for one-way full-duplex MIMO relaying systems," *Proceedings of the Tenth International Symposium on Wireless Communication Systems (ISWCS)*, Aug. 2013.

[26] I. Krikidis, H. Suraweera, P. Smith, and C. Yuen, "Full-duplex relay selection for amplify-and-forward cooperative networks," *IEEE Transactions on Wireless Communications*, Dec. 2012.

[27] O. Taghizadeh and R. Mathar, "Cooperative strategies for distributed full-duplex relay networks with limited dynamic range," in *International Conference on Wireless for Space and Extreme Environments (WiSEE), 2014 IEEE*, Noordwijk, Netherlands.

[28] T. Riihonen, S. Werner, and R. Wichman, "Optimized gain control for single-frequency relaying with loop interference," *IEEE Transactions on Wireless Communications,*, 2009.

[29] L. Jimenez Rodriguez, N. Tran, and T. Le-Ngoc, "Optimal power allocation and capacity of full-duplex AF relaying under residual self-interference," *IEEE Wireless Communications Letters*, April 2014.

[30] H. Suzuki, T. V. A. Tran, I. B. Collings, G. Daniels, and M. Hedley, "Transmitter noise effect on the performance of a MIMO-OFDM hardware implementation achieving improved coverage," *IEEE J. Sel. Areas in Communication*, vol. 26, pp. 867–876, Aug. 2008.

[31] W. Namgoong, "Modeling and analysis of nonlinearities and mismatches in AC-coupled direct-conversion receiver," *IEEE Trans. Wireless Commun.*, vol. 47, pp. 163–173, Jan. 2005.

[32] B. Day, A. Margetts, D. Bliss, and P. Schniter, "Full-duplex bidirectional MIMO: Achievable rates under limited dynamic range," *IEEE Transactions on Signal Processing*, Jul. 2012.

[33] M. Duarte, C. Dick, and A. Sabharwal, "Experiment-driven characterization of full-duplex wireless systems," *IEEE Transactions on Wireless Communications*, December 2012.

[34] C. Dang, L. Jimenez Rodriguez, N. Tran, S. Shelly, and S. Sastry, "Secrecy capacity of the full-duplex AF relay wire-tap channel under residual self-interference," in *IEEE Wireless Communications and Networking Conference (WCNC)*, March 2015.

[35] R. Lorenz and S. P. Boyd, "Robust minimum variance beamforming," *IEEE Transactions on Signal Processing*, vol. 53, May 2005.

[36] D. Michalopoulos, H. Suraweera, G. Karagiannidis, and R. Schober, "Amplify-and-forward relay selection with outdated channel estimates," *Communications, IEEE Transactions on*, May 2012.

[37] B. Zhong, D. Zhang, Z. Zhang, Z. Pan, K. Long, and A. Vasilakos, "Opportunistic full-duplex relay selection for decode-and-forward cooperative networks over rayleigh fading channels," in *IEEE International Conference on Communications (ICC)*, June 2014.

[38] X. Rui, J. Hou, and L. Zhou, "Decode-and-forward with full-duplex relaying," *Int. J. Commun. Syst.*, vol. 25, no. 2, Feb.